



THE EFFECT OF GRAPHITE PROPERTIES ON THE RATE OF MnO REDUCTION FROM HIGH CARBON FERROMANGANESE SLAG

J. Safarian, L. Kolbeinsen, S. Gaal¹ and G. Tranell¹

Department of Materials Science and Engineering, Norwegian University of Science and Technology
Alfred Getz Vei 2, Trondheim, Norway

E-mail: jafar.safarian@material.ntnu.no and Leiv.Kolbeinsen@material.ntnu.no

¹SINTEF Materials and Chemistry, Alfred Getz Vei 2, Trondheim, Norway

E-mail: Sean.Gaal@sintef.no and Gabriella.M.Tranell@sintef.no

ABSTRACT

The effect of carbon material properties on the rate of MnO reduction from ferromanganese slag by solid graphite was investigated. A sessile drop technique was used to study the reduction rate of a synthetic slag containing 45 wt% MnO at 1500 and 1600 °C. Different types of graphite substrates were used and the contact angle between slag droplets and substrate were measured in-situ. Moreover, the slag droplet volume during the interaction with the graphite substrates was calculated and normalised. The mathematical relationship between the slag density during the reduction and the normalised slag droplet volumes during the reduction were derived and the MnO reduction curves were then calculated. A method for measuring the slag reactivity of solid carbon was defined and used to qualify the propensity of the different graphites to react with the liquid slag. Some supplementary studies such as manganese evaporation measurement and EPMA analysis for determining the extent of MnO reduction were also carried out. It was observed that there is not a significant difference in the wetting angle of the graphite substrates by the slag, and the wetting is not changed within the temperature range of 1500-1600°C. However, the changes in the contact angle during the slag reduction at 1600°C are more than at 1500°C. The kinetics of MnO reduction is dependent on the type of graphite and it is more dependent on the graphite properties at lower temperatures. On the other hand, the dominant properties of graphite on the reduction rate vary with temperature. A multivariate analysis on the graphite properties and the parameters related to the slag reactivity indicated that the kinetics of MnO reduction is mainly dependent on the temperature, and then on the graphite properties. It was also found that at 1500 °C the surface area and the CO₂ reactivity are the most important graphite properties for the slag reduction, suggesting that the reactivity of carbon is rate controlling at 1500 °C. However, the porosity related parameters are the most important graphite properties at 1600 °C, suggesting that CO gas desorption is rate controlling at high temperatures.

1. INTRODUCTION

The interaction of solid carbon material with liquid slag is one of the critical reactions in many metallurgical processes. In a submerged electric arc furnace which is used for high-carbon ferromanganese (HC_FeMn) production, manganese oxides in the burden are reduced to MnO directly by CO gas. Subsequently, manganese metal is produced through the interaction of a high MnO containing molten silicate slag with carbon in the coke bed area according to this reaction:



The carbothermic reduction of MnO from slags has been studied from different points of view over the past decades and a vast quantity of data has been determined experimentally. From a thermodynamic point of view the direct reduction of MnO by CO is impossible due to the low equilibrium constant for the reduction reaction, which even at 2000K is not higher than about 7×10^{-4} . Thus, in the HC_FeMn process MnO is only reduced by carbon according to equation (1), where the reductant can be solid carbon or dissolved carbon in the metal phase (Mn-Fe-C alloy).

The kinetics of the MnO reduction by carbon and the effects of different parameters have been studied by several investigators [1-11]. These studies have mainly been conducted in graphite crucibles, with different metal compositions involving Fe-C, Mn-C and Fe-Mn-C alloys. In the past, several mechanisms for MnO reduction have been proposed. For example, it has been observed that stirring has no effect on the kinetics of MnO reduction, while the reduction rate is extensively sensitive to the temperature. Therefore, it has been concluded that the reaction kinetics are not controlled by diffusion in the bulk of the metal and slag phases, suggesting that the rate of MnO reduction from slag is controlled by chemical reaction [1-10]. But, based on the observation that the gas composition affects the kinetics, it has recently been proposed that MnO reduction is mix-controlled involving both chemical reaction and CO mass transfer in the gas phase [11]. The mechanism of MnO reduction from slags by dissolved carbon in liquid iron is well known [3, 5, 6, and 10]. According to this mechanism MnO is reduced by Fe to Mn and FeO at the slag/metal interface. Subsequently, FeO is reduced by CO gas to Fe and CO₂ gas at the slag/gas bubble interface, followed by the regeneration of CO gas via the Boudouard reaction with dissolved carbon at the metal/gas bubble interface. In contrast, the mechanism of MnO reduction by solid carbon and dissolved carbon in liquid manganese is still unknown and more investigations are required.

A few studies have recently been carried out to find the effects of the carbonaceous material properties on the kinetics of the simultaneous reduction of MnO and SiO₂ from silicate slags at 1600 °C [12, 13]. It has been observed that the reductant type influences the SiO₂ reduction significantly, while it does not have a large effect on the MnO reduction. The objective of the present study is focusing more to investigate any possible relations between the kinetics of the carbothermic reduction of MnO and the properties of carbon materials. In this case, different pure graphites (with low ash contents) are used as the carbon materials, and the effects of their properties on the MnO reduction kinetics from a master slag are investigated.

2. EXPERIMENTAL PROCEDURES

As the main focus of the study involved the role of graphite properties on the slag reduction, a part of the study was dedicated to characterisation of the different properties of the graphite. The applied methods for graphite characterisation are described in section 2.1.

In order to study the kinetics of MnO reduction from high carbon ferromanganese slag, a synthetic slag was made and then reduced by different graphites with a sessile drop wettability technique. The materials preparation procedures and the experimental set up are described in section 2.2.

2.1 Characterisation of Graphites

Six different purified graphites with more than 99.9 wt% fixed carbon content (ash content less than 0.1 wt%) were used in this study. The properties of these graphites were characterised as described below.

2.1.1 Physical properties

Mercury porosimetry was used in order to determine the porosity related parameters such as total pore volume per unit weight, average pore diameter, porosity and the bulk density. Moreover, the specific surface area of the graphites was measured by BET using nitrogen gas as the surface adsorbate agent.

2.1.2 Structural parameters

In order to determine the structural parameters of the graphites, X-ray diffraction (XRD) was used. In this case, the graphites were milled to less than 44 µm (through a 325 mesh standard sieve). Then they were mixed with 10 wt% high purity silicon powder as an internal standard [14]. The samples were scanned at a wavelength of 1.540562 Å (Cu K α X-ray), with a step size of 0.02°, at 0.5 s/step. The obtained XRD spectrums were processed according to the newly developed procedure for carbon materials characterisation by Iwashita et al. [14]. Using software, a mathematical function was fitted to correct each diffraction profile, and the backgrounds were removed. As the result, peak positions for carbon (002) and the full width of half maximum (FWHM) were determined. Subsequently, the structural parameters such as carbon layer spacing (d_{002}) and

the average crystallite size ($L_{C(002)}$) were calculated by applying Bragg's law and the Outlined method by Iwashita et al.[14], respectively.

2.1.3 CO_2 reactivity

CO_2 reactivity is a parameter frequently used for the characterisation of carbon based reductants in various metallurgical processes. CO_2 reactivity describes the propensity of carbonaceous material to react with CO_2 gas according to the Boudouard reaction:



In this study, the CO_2 reactivity for all graphites was measured at 1000 °C in a 100% CO_2 atmosphere. The reactivity measurements were carried out in a TGA where an initial 50 grams of material with 1.68-3.36 mm particle size was heated up in argon to 1000 °C and held until no mass loss was recorded. At this point the furnace atmosphere was replaced with CO_2 with a flow rate of 5 litre per minute for 3 hours. The mass loss changes during the experiment were subsequently converted to the reacted fraction X of the sample mass. The changes in the reacted fraction with time (dX/dt), which were linear during the whole of the reaction time, were calculated and used to characterise as the graphite reactivity.

2.2 Slag Reduction

The interactions between different graphites and a master slag were investigated using a sessile drop approach. The materials preparation and the details of the experiments are described below.

2.2.1 Materials preparation

The graphite materials were in the form of a block, which were cut into slices 4 mm thick. Graphite discs with a diameter of 10mm were then cut with a core drill from these slices. The surface of these discs was polished using SiC paper to 1200 grit size (14 μ m). For preparing the master slag, high purity slag powders of CaO, MgO, SiO_2 and Al_2O_3 were mixed and then melted in a graphite crucible in air. The obtained slag was then crushed in a disc mill and the slag powder was mixed with pure MnO powder, and then was melted in a platinum crucible in air. The final master slag composition in weight percent was 45%MnO-13.4%CaO - 25% SiO_2 -10% Al_2O_3 -6.6%MgO as measured by XRF.

2.2.2 Furnace construction and experimental details

A horizontal tube furnace was used in order to study the wetting properties in the sessile drop method. A schematic diagram of the experimental set up is shown in Figure 1. The graphite substrate was located in the graphite sample holder and a 40 mg slag particle was put on the polished surface of the substrate. The furnace chamber was evacuated initially, and then the furnace was heated up slowly in an argon atmosphere. The furnace was heated to 950 °C in approximately 10 minutes, followed with a rapid heating rate of 120°C/min to the experiment temperature. In the present study, the isothermal reduction of the slag was investigated at 1500°C and 1600°C for 60 and 30 minutes, respectively. The temperature was controlled using a Keller PZ40 two colour pyrometer operating from 900-2400°C focused on the edge of the graphite sample holder (Fig. 1). A fire-wire digital video camera (Sony XCD-SX910CR) with a telecentric lens (Navitar 1-50993D) was used to record images from the sample at 960x1280 pixels. In the experiments, drop images were captured every second and then they were processed by software to measure some parameters such as contact angle, contact area, drop volume and surface tension.

2.2.3 Supplementary studies

After completion of the wettability experiments, the samples were quenched. The weight of the solidified slag drops were measured, as there was no sticking between graphite and slag after the experiments. The slag drops were then mounted in epoxy and prepared for electron probe X-ray microanalysis (EPMA) with wavelength dispersive spectrometers.

Manganese metal which is produced in Reaction (1) evaporates due to its high vapour pressure. In order to determine the rate of Mn evaporation rates, the sessile drop wetting technique was also used to evaporate a manganese droplet at 1500°C and 1600°C. In this case, pure electrolytic manganese on an alumina substrate was evaporated in an argon atmosphere with an oxygen partial pressure of 1.0×10^{-25} atm (Cambridge Sensotec Rapadox 2100).

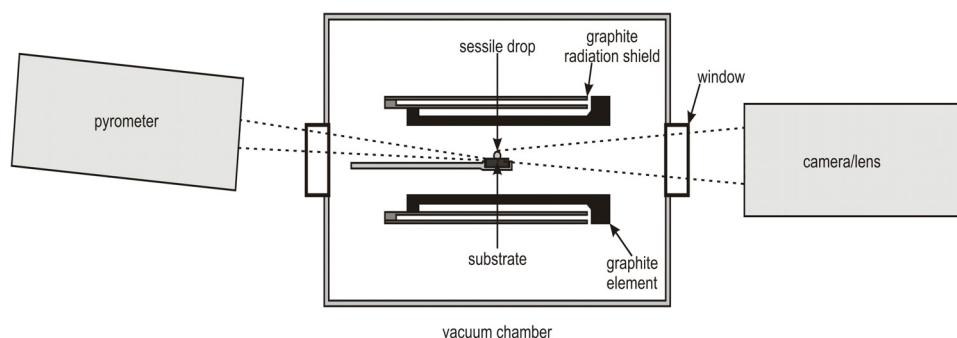


Figure 1: Schematic diagram of the experimental set-up.

3 RESULTS AND DISCUSSION

3.1 Properties of Graphites

The measured properties of the graphites are summarised in Table 1. As we can see all of the graphites have at least 2 different properties from the other graphites. It is possible to compare the graphites by considering the main differences. For example, graphites A and B are different mainly in porosities and the size of the pores. However, the pore size, the surface area and the grain size are different between graphites D and F. Although it is possible to make more comparisons between the graphites in this way, it is very difficult to come to a definite conclusion from so many properties with regards to their possible effects on the slag reduction kinetics. Therefore, in the present study a multivariate analysis was applied to capture the most important properties of the graphite on the slag reduction kinetics (section 3.5).

3.2 The Rate of MnO Reduction

Figure 2 shows the changes in the contact angle between the slag droplet and different graphite substrates, θ , at 1500°C and 1600°C. This figure shows that the contact angle decreases during the interaction of graphites with slag, indicating that the interfacial tensions between the slag droplet and the graphite substrates and Ar gas are changed during MnO reduction. Considering the initial contact angles, the wetting of graphite substrates with the same slag (containing 45wt%MnO) are approximately the same at the experimental temperatures with maximum 5 degrees changes at each temperature. However, the contact angle changes during MnO reduction are not the same for different graphite substrates, and the changes at 1600°C are higher than 1500°C. The contact angle related parameters consisting of the initial contact angle θ_i , the final contact angle θ_f , total change in the contact angle ($\Delta\theta$) and the average change in the contact angle $(-d\theta/dt)_{av}$ are summarised in Table 2.

Although the rate of change in the contact angle can be used to study the kinetics of slag reduction [15], it is not a satisfactory parameter to study the MnO reduction. Comparing $\Delta\theta$ and $-d\theta/dt$ value in Table 2 with the total changes in the slag droplet masses, which shows the extent of MnO reduction, indicates that there is not any meaningful relation between these parameters. Therefore, it seems to be impossible to extract the re-

Table 1: The measured properties of the graphites

Graphite no.	Cumulative pore volume ($\times 10^{-2} \text{ cm}^3/\text{g}$)	Average pore diameter (μm)	porosity (%)	Bulk density (g/cm^3)	Surface area (cm^2/g)	Interplanar distance $d_{(002)}$, nm	Crystallite size $L_{c(002)}$ nm	Average grain size (μm)	CO_2 reactivity ($1/\text{min}$)
A	10.5	2.5	18.3	1.742	4000	0.3364	55.335	10	0.0007
B	8.6	2.3	15.3	1.779	4000	0.3366	50.319	10	0.0003
C	13.8	2.58	22.9	1.659	7000	0.3358	57.878	10	0.001
D	7.2	2.72	13.4	1.858	3000	0.3370	42.530	10	0.0004
E	8.8	2.06	15.8	1.779	6000	0.3377	32.726	5	0.0011
F	6.4	0.66	12.1	1.885	5000	0.3373	44.279	5	0.0006

Table 2: The contact angle related parameters, the total slag mass change and the final MnO content of slag for reduction by different graphite substrates at 1500°C and 1600°C

Graphite no.	Reduction temperature (°C)	Total slag mass changes (mg)	Start θ (degree)	End θ (degree)	$\Delta\theta$ (degree)	$(-d\theta/dt)_{av}$ (degree/min)	MnO content after reduction (wt%)
A	1500	9.2	158.9	154.8	4.1	0.026	28.8
B	1500	8.6	156.5	154.5	2	0.0129	31.1
C	1500	11.4	154.7	151.5	3.2	0.0653	23.6
D	1500	13.3	155.9	149.8	6.1	0.0777	18.6
E	1500	12.9	159.1	157.2	1.9	0.0168	19.54
F	1500	10.9	158.8	152.1	6.7	0.1235	25.1
A	1600	8.7	156.6	151.2	5.4	0.1564	30.1
B	1600	9.3	157.5	153.8	3.7	0.1164	28.4
C	1600	11.5	155.3	146.5	8.8	0.2904	22.6
D	1600	11.4	156.7	147.4	9.3	0.3142	23.2
E	1600	11	152.8	146.4	6.4	0.183	24.1
F	1600	11.1	156	147.5	8.5	0.2687	23.2

duction rates of slags from the rate of the changes in the contact angle.

An alternative option to study the kinetics of MnO reduction from a slag drop is to measure the changes in the drop volume during the reduction. In this case, the changes in the drop slag volume (V_s) were normalized considering initial drop volume ($V_{s,i}$) by calculating the changes in the $V_s/V_{s,i}$ ratio for slag reduction by graphite substrates at 1500°C and 1600°C. It is worth mentioning that the volume of the graphite substrate which is consumed by the slag reduction is very small and it has no effect on the calculations of the slag volume. For example, for the slag reduction with graphite E at 1500°C, the average contact area with graphite is about 1.0445 mm² and the total reduced MnO is 12.9 mg. Considering that the graphite is consumed uniformly in the contact area with slag, a height of 15 μm of graphite is consumed for the reduction and it is negligible in comparison with the slag height and volume. The latter parameters are 2.53 mm and 10.3 mm³ respectively, after 60 minutes reduction to 19.54 wt% MnO.

If the density of slag (ρ_s) is constant during the MnO reduction (independent of MnO content), the changes in $V_s/V_{s,i}$ can be directly compared to the slag mass changes, and mass loss change can consequently be considered as the rates of MnO reduction. In order to determine the possible changes in the slag density during MnO reduction, some wetting experiments were carried out with shorter reduction times. The slag masses were measured before and after each experiment and the densities were calculated regarding the drop volume measurements. It was found that there is a linear relationship between the slag density and the changes in $V_s/V_{s,i}$ ratio during MnO reduction as is illustrated in Figure 3. And this relationship gives:

$$\rho_s = 1.26 (V_s/V_{s,i}) + 1.766 \quad \text{at } 1500 \text{ }^\circ\text{C} \quad (3)$$

$$\rho_s = 1.04 (V_s/V_{s,i}) + 2.05 \quad \text{at } 1600 \text{ }^\circ\text{C} \quad (4)$$

Regarding the fact that products of Reaction 1 leave the slag droplet, the MnO content of the drop can be calculated by a mass balance using the initial slag mass ($m_{s,i}$) and the slag mass at a given reduction time (m_s):

$$\text{wt}\% \text{MnO} = \frac{(\text{wt}\% \text{MnO}_i \cdot m_{s,i}) - (m_{s,i} - m_s)}{m_s} \quad (5)$$

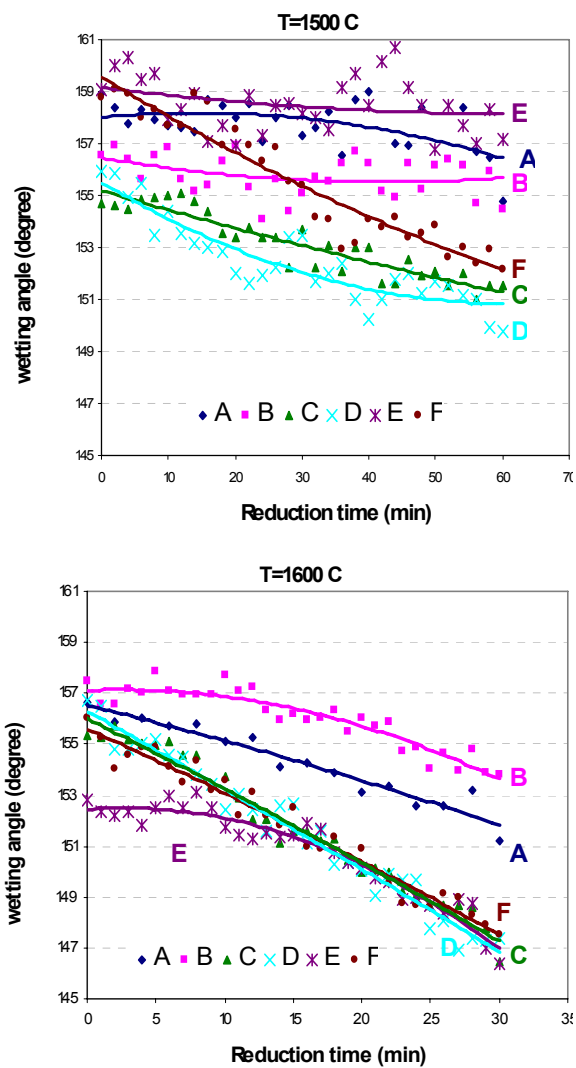


Figure 2: The changes in the contact angle, θ , between the slag droplet and graphite substrates at 1500°C and 1600°C.

and

$$m_s = V_s \rho_s \quad (6)$$

where $wt\%MnO_i$ is the initial MnO content of slag which was 45 wt% in this study. All the ratios of $V_s/V_{s,i}$ were converted to the MnO content of slag with equations (3) to (6). The obtained reduction curves are illustrated in Figure 4, and they indicate that the reduction rate is affected by the type of graphite at a given temperature. The differences in the reduction rates at 1500°C are more significant than 1600°C, indicating that carbon material properties are more important at lower temperatures. On the other hand, the relative order of the reduction curves is not the same at different temperatures. It may indicate that the kinetics of MnO reduction is dependent on the different parameters of solid carbon material, and the role of these parameters is changing with the temperature.

3.3 The Slag Reactivity Evaluation

Although some experimental techniques have been developed to study the propensity of carbon to react with gases (like CO₂ reactivity test), no experimental technique has been suggested to measure the propensity of carbonaceous materials to react with liquid slags. A method which is measuring the slope of the reduction curve, $-d(wt\%MnO)/dt$, at fixed MnO contents of slag is used as the slag reactivity parameter in the present study.

The slag reactivity of all graphites was calculated at 40 and 35 wt%MnO, at both experimental temperatures. The reactivity results and the re-

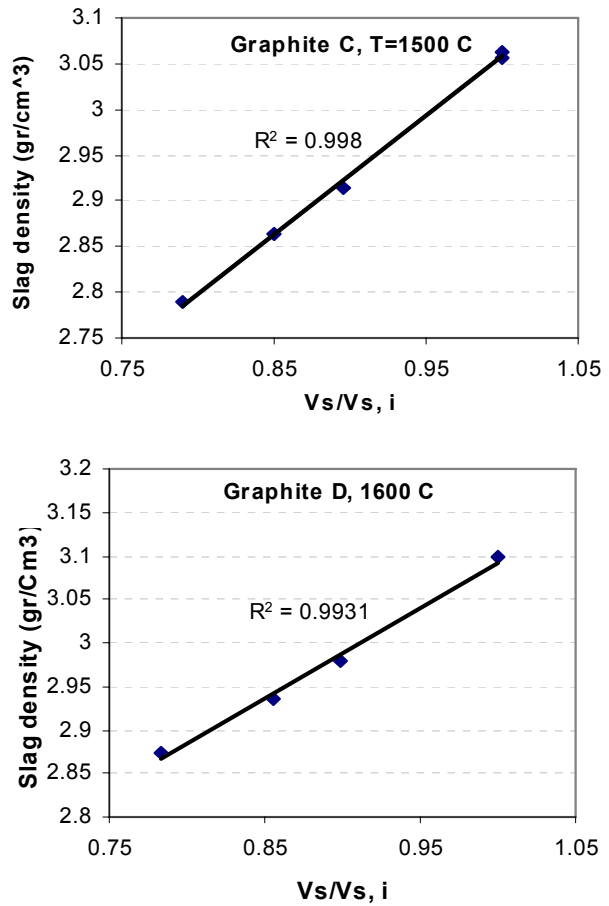


Figure 3: The relationship between the slag density and $V_s/V_{s,i}$ ratio at 1500 and 1600 °C. The points were obtained by the slag reduction on graphites C and D

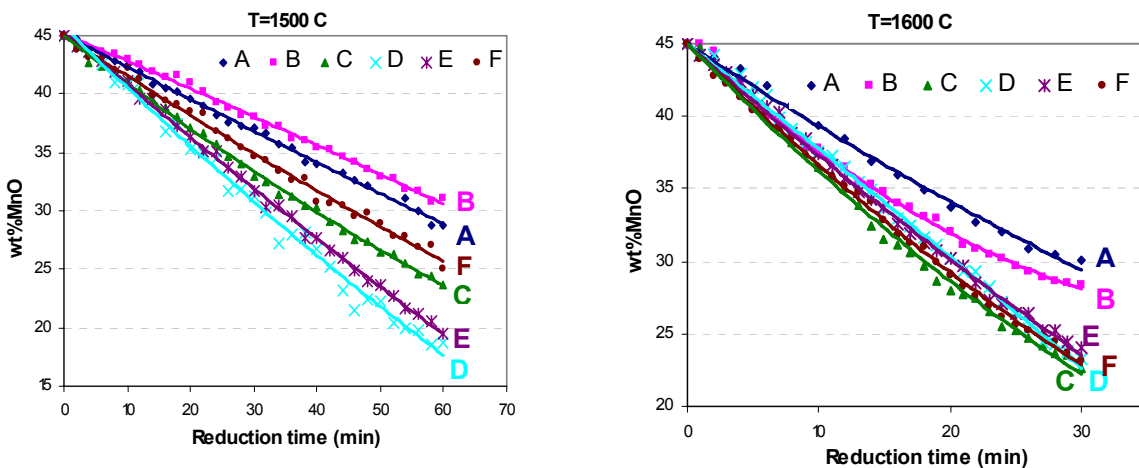


Figure 4: The MnO reduction from slag droplet by different graphites at 1500 and 1600 °C

quired time to achieve these fixed MnO contents are summarised in Table 3. As we can see, the slag reactivity at 1500°C for both 40 and 35wt%MnO are the same, with completely linear reduction patterns. In contrast, these values at 1600°C are different due to the appearance of a curvature in the reduction rates. The slag reactivity at 1600°C is about two times higher than 1500°C, indicating that the temperature is a very important factor. Table 3 shows also that the highest reactivity are obtained for graphites D at 1500°C, while graphite C has the highest reactivity at 1600°C.

Table 3: The reactivity related parameters for MnO slag reduction by different graphites at 1500 and 1600 °C

Graphite	Reduction temperature (°C)	Required time to reach 40 wt%MnO (min)	Required time to reach 35 wt%MnO (min)	Reactivity at 40wt% MnO (-wt%MnO/min)	Reactivity at 35wt% MnO (-dwt%MnO/dt)
A	1500	18.3	36.8	0.2714	0.2684
B	1500	22	42.9	0.2334	0.2459
C	1500	12.3	25.5	0.3936	0.3646
D	1500	10.5	21.1	0.4732	0.4647
E	1500	11.4	23.0	0.4350	0.4304
F	1500	14.5	29.7	0.3368	0.3216
A	1600	8.7	18.2	0.5512	0.5056
B	1600	6.5	14.2	0.7134	0.8278
C	1600	5.5	11.5	0.8714	0.7994
D	1600	6.9	13.7	0.7297	0.7433
E	1600	6.4	13.1	0.7648	0.7265
F	1600	5.8	12.1	0.8296	0.7666

3.4 Manganese Evaporation Consideration

In order to determine the manganese evaporation rates, the changes in the manganese metal droplet volume (V_{Mn}) were converted to the slag droplet mass (m_{Mn}). In this case, the pure manganese metal density at 1500 and 1600°C was calculated as 5.994 and 6.086, respectively. The relationship between the density of pure Mn and temperature is [16]:

$$\rho = \rho_m + A (T - T_m) \quad (7)$$

where ρ_m (=7.56 g/cm³) and ρ are the pure manganese densities at melting point (T_m =1246°C) and temperature T , and A is a temperature dependent factor (A =0.00092 g/cm³ K).

Figure 5 shows the changes in the mass of the manganese drop at the experimental temperatures, and it indicates that the manganese evaporation rate is 3.77 and 5.4 mg/min for 1500°C and 1600°C, respectively, which is approximately constant. Figure 6 shows the highest rates of Mn production in the slag reduction experiments which are for graphites D and C at 1500 and 1600°C, respectively. Graphite D has an average manganese production rate 0.179 mg/min, while graphite C has a maximum Mn production rate of 0.4 mg/min in the beginning. Comparing Figures 5 and 6 gives this important result of having much higher rates of Mn evaporation than the rates of Mn production in the slag reduction experiments. The micro_structural studies by EPMA confirmed that there is no metal phase at the reaction interface between the slag and graphite. It is worth mentioning that only a few very small spherical metal particles were observed in the droplet (smaller than 1 µm), and their analysis was not possible due to their small size.

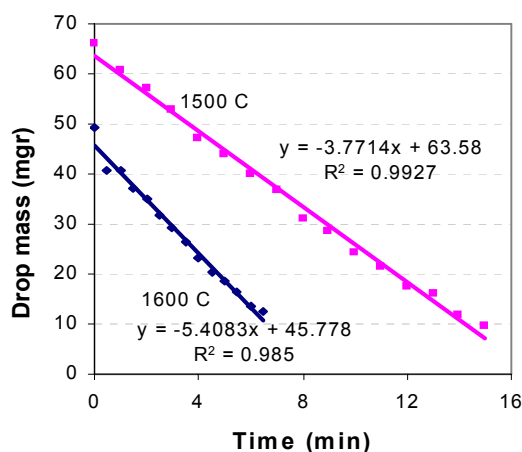


Figure 5: The changes in the Mn drop mass in Ar atmosphere at 1500°C and 1600 °C

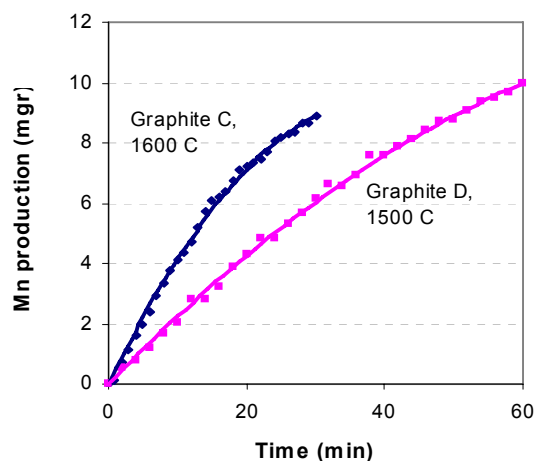


Figure 6: The rate of Mn production from slag drop reduction by graphites E and C at 1500°C and 1600 °C, respectively.

3.5 Multivariate Analysis of Data

In order to determine the possible relationships between the kinetics parameters of MnO reduction (slag reactivity and contact angle related parameters) and the graphite properties, a multivariate analysis was applied using the Unscrambler® software version 6.

The principle component analysis (PCA) was used to study the graphite materials and their properties (Table 1). The score plot which can be used to study the differences and similarities among the graphites is shown by open symbols in Figure 7. The score plot shows that the graphite materials A to F have different properties, because they are not very close to each other. However, the similarities in graphites A, B, and D are more than the other samples, and the highest differences are between graphites C and F. The loading plot, solid symbols in Figure 7, shows the differences and similarities between the properties of the graphites. The loading plot indicates that the cumulative pore volume is the same parameter as the porosity due to the overlapping of their points. However, bulk density is a completely different parameter and it has an inverse relationship with the porosity, because they are located in different areas and on a line crossing the origin. The loading plot also illustrates that the CO₂ reactivity and the specific surface area are close parameters, and it may indicate that CO₂ reactivity is mainly dependent on the surface area for graphite.

The graphite properties in Table 1, including the experimental temperatures were considered as X-variables (predictors) and the slag reduction kinetics parameters (Tables 2 and 3) were considered as the Y-variables (respon-

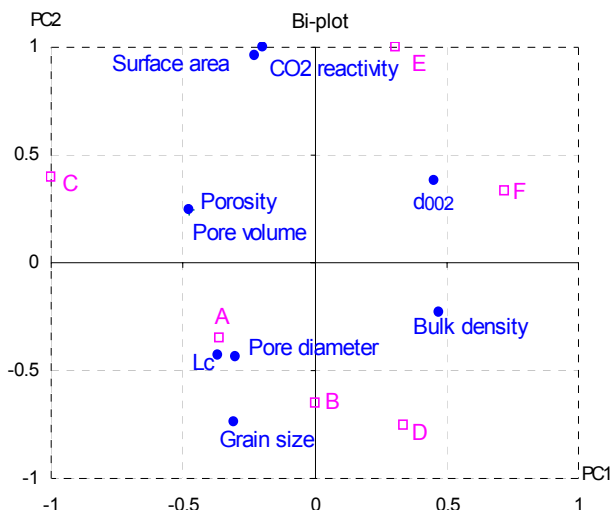


Figure 7: The score and loading plots for the graphite materials and their properties. Score plot: solid symbols, loading plot: open symbols

es). Then the Partial Least Squares regression (PLS) method was applied to study the relationships between X and Y variables. Figure 8 shows the X and Y loading results for all the variables. It indicates that the slag reactivities at 40 and 35 wt% MnO (SR40 and SR35) have very close positions and they are affected mainly by the temperature. They are also in the same area with the specific surface area and the CO₂ reactivity, indicating they are affected by these parameters. The measured Y-variables were plotted against the predicted Y values using the PLS model. It was observed that there is good agreement between the model and the data as is illustrated in Figure 9 for SR40. The correlations for the slag reactivity were the best, followed by the required times to reach 40 and 35 wt% MnO (t40 and t35), the average contact angle rate of change ($\Delta\theta/dt$), the total θ changes (Tot- θ) and the final MnO content of slag (%MnO), respectively. The importance of the different X-variables for predicting Y-variables are shown in Figure 10 and it indicates that the temperature is the most important parameter for the slag reactivity. It shows also that the slag reactivity is affected by all the properties of graphite listed in Table 1.

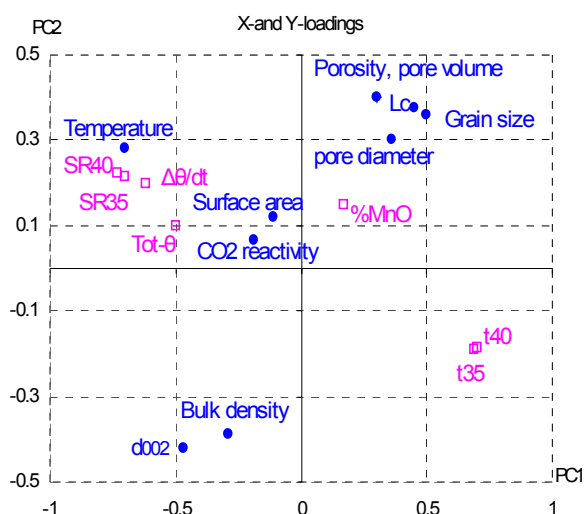


Figure 8: The loading plot for the graphite properties and temperature (solid symbols) and the slag reduction kinetics properties (open symbols)

The PLS model was also used to study the effect of graphite properties (X-variables) on the slag reactivity (Y-variable) at 1500°C and 1600°C separately. Considering all the graphite samples, no relation was found between the X and Y variables at each temperature. In order to find any exception among the samples, the calculations were repeated by considering only 5 graphites as the samples. It was found that there is only a good correlation between the measured and predicted slag reactivity by keeping only specific graphite out of the calculations at each temperature. Keeping graphite D out of model calculations at 1500°C, a good correlation was observed between the measured and predicted slag reactivities. Figure 11 shows the important graphite properties on the SR40 at 1500°C and it indicates that the specific surface area and CO₂ reactivity

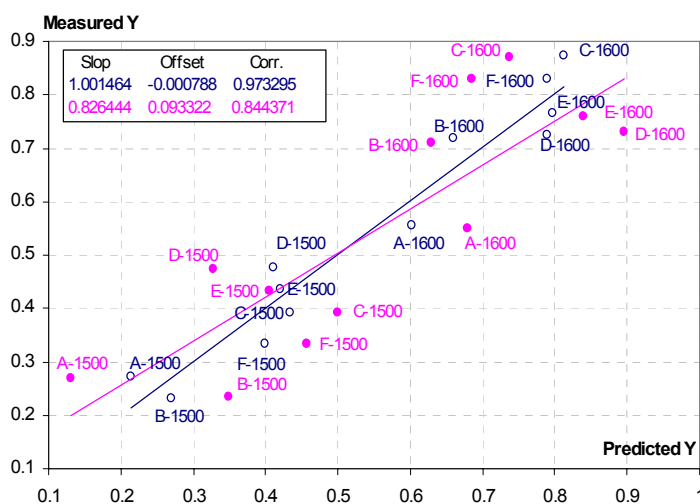


Figure 9: The prediction/measured plot for the slag reactivity at 40 wt% MnO (SR40). Open symbols: measured, and Solid symbols: prediction

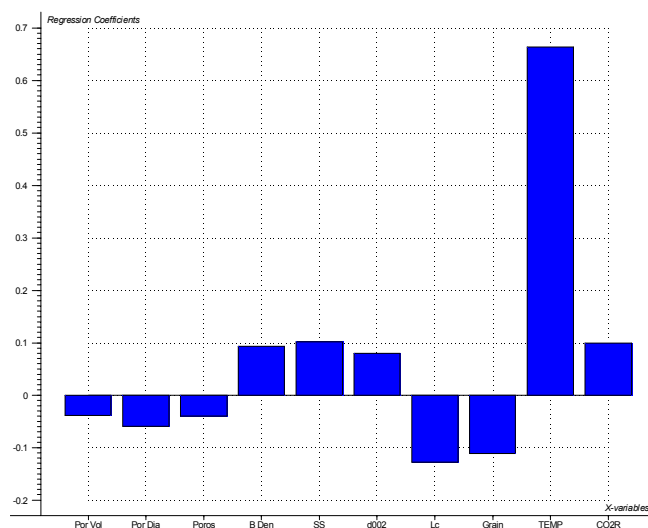


Figure 10: Weighted regression coefficients for the slag reactivity (SR40) affecting parameters

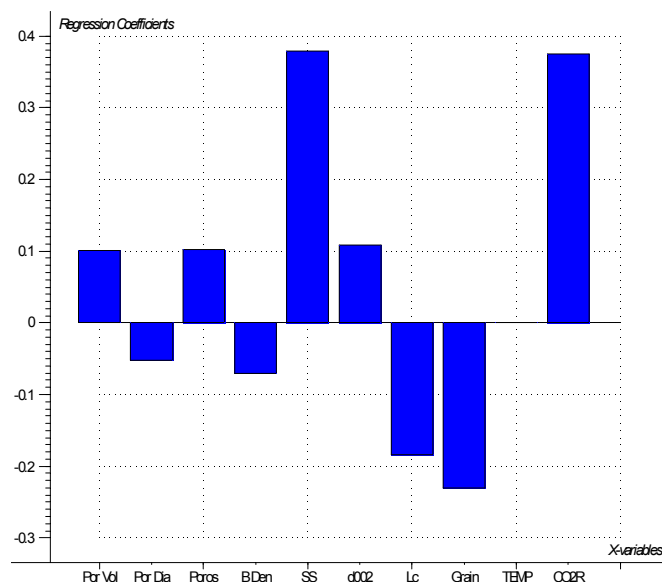


Figure 11: Weighted regression coefficients for the slag reactivity (SR40) affecting parameters at 1500°C for all graphite samples except D

are the most important parameters at this temperature. This relation between the CO₂ reactivity and the slag reduction kinetics may indicate that the reactivity of reactants of Reaction 1 is the rate controlling step at 1500°C. The model calculations at 1600°C indicated that the best correlation between the measured and predicted SR40 is obtained if graphite C is kept out of the samples. It was found that the most important graphite properties for slag reactivity are the structural properties and physical properties of graphite (Figure 12). As we can see specific surface area and CO₂ reactivity are not important at 1600°C, while at 1500°C they are the most important parameters. The dependence of the slag reduction kinetics on the porosity related parameters at 1600°C may show that at this temperature the reduction rate is more dependent on the desorption of CO gas which is produced from chemical Reaction 1.

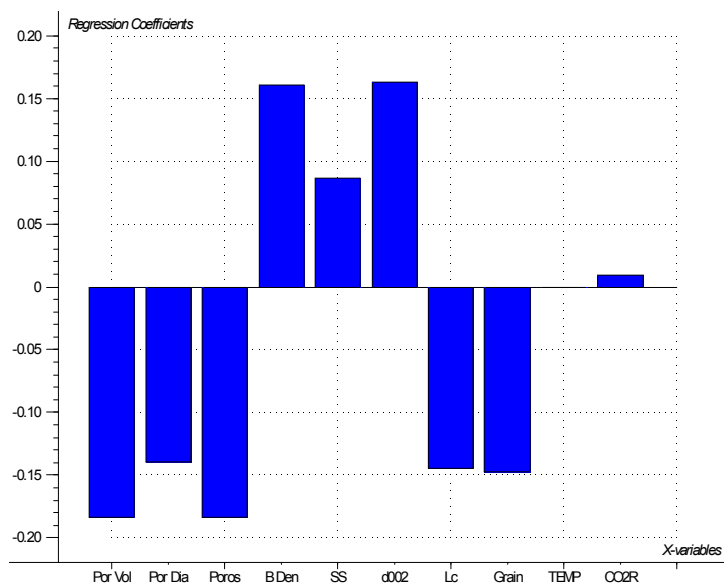


Figure 12: Weighted regression coefficients for the slag reactivity (SR40) affecting parameters at 1600°C for all graphite samples except C

4. CONCLUSIONS

1. The wetting of different graphites by a slag with fixed MnO content is approximately the same, and the wetting does not change significantly within the temperature in the range of 1500-1600 °C.
2. The kinetics of slag reduction in a sessile drop wetting technique can be studied by normalising the changes in the drop volume and applying the related density change equations.
3. The kinetics of MnO reduction from slag by graphite is dependent on the graphite properties and the importance of these properties at 1500 °C is higher than at 1600°C.
4. A method was applied to measure the slag reactivity of carbon materials; it indicated that the slag reactivity of graphite at 1600°C is much higher than at 1500°C.
5. The slag reactivity of graphite is mainly dependent on the temperature and the graphite properties are in the lower order of importance.
6. The kinetics of MnO reduction from slag is affected by the graphite properties and the important properties change with changing temperature. At 1500°C the surface area and CO₂ reactivities are the most important parameters and at 1600°C the porosity related parameters and the structural properties are more important.
7. The rate of MnO reduction from slag is controlled by the reactivity of carbon material at lower temperatures and by the CO desorption at higher temperatures.

REFERENCES

- [1] Tarby, S. K. and Philbrook, W. O., "The rate and mechanism of the reduction of FeO and MnO from silicate and aluminate slags by carbon-saturated iron" Trans. AIME, 239, 1967, pp.1005-1017.
- [2] Daines, W. L. and Pehlke, R. D., "Kinetics of manganese oxide reduction from basic slags by carbon dissolved in liquid iron", Metallurgical Transactions, 2, 1971, pp. 1203-1211.
- [3] Pomfret, R. J. and Grieveson, P., "Kinetics of fast initial stage of reduction of MnO from silicate slags by carbon in molten iron", Ironmaking and Steelmaking, No. 5, 1978, pp. 191-197.
- [4] Shimoo, T., Ando, S. and Kimura, H., "Rates of MnO reduction from silicate slags with solid carbon", J. Japan Inst. Metals, 48, 1984, No. 9, pp. 922-929.

- [5] Upadhyaya, K., "The kinetics and mechanism(s) of manganese oxide reduction from liquid slag by carbon dissolved in iron", ISS Transactions, 7, 1986, pp. 1-6.
- [6] Xu, K., Jiang, G., Ding, W., Gu, L., Guo, S. and Zhao, B., "The kinetics of reduction of MnO in molten slag with carbon saturated liquid iron", ISIJ International, 33, 1993, No. 1, pp. 104-108.
- [7] Skjervheim T. A., "Kinetics and mechanisms for transfer of manganese and silicon from molten oxide to liquid manganese metal", Dr. Ing. Dissertation, NTH, Trondheim, Norway, 1994.
- [8] Tangstad, M., "The high-carbon ferromanganese process – coke bed relations", Dr. Ing. Dissertation, NTH, Trondheim, Norway, 1996.
- [9] Olsø, V., Tangstad, M, and Olsen, S.E., "Reduction kinetics of MnO-saturated slags", Proc. INFACON 8, The Chinese Society for Metals, Beijing, China, 1998, pp. 279-283.
- [10] Guo, S. Q., Jiang, G. C., Xu, J. L., Xu, K. D., "Kinetics of reduction of MnO in molten slag with carbon undersaturated liquid iron", J. Iron & Steel Res. Int., 7, 2000, No. 1, pp. 1-5.
- [11] Yastreboff, M., Ostrovski, O. and Ganguly, S., "Effect of gas composition on the carbothermic reduction of manganese oxide", ISIJ Int., 43, 2003, No.2, pp.161-165.
- [12] Berg, K., Olsen, S. E., "Kinetics and mechanism for the carbothermic reduction of MnO and SiO₂ from liquid slags", SINTEF internal report (STF24 A04531), 2004.
- [13] Gaal S., Berg K., Tranell G., Olsen S.E., and Tangstad M., "An investigation into aspects of liquid phase reduction of manganese and silica containing slag", 7th International Conference on Molten Slags, Fluxes and Salts, Cape Town, South Africa, Jan. 2004, pp. 651-657.
- [14] Iwashita, N., Park, C. R., Fujimoto, H., Shiraishi, M. and Inagaki, M., "Specification for a standard procedure of X-ray diffraction measurements on carbon materials", CARBON, 42, 2004, pp. 701-714.
- [15] Hayes, P. C., Okongwu, D.A. and Toguri, J., "Some observations of the reactions between molten oxides and solid carbon", Canadian Metallurgical Quarterly, Vol. 34, No. 1, pp. 27-36.
- [16] Iida, T. and Guthrie, R. L., "The physical properties of liquid metals", Clarendon Press, Oxford, 1988, pp. 70-73.